International Journal of Engineering Research and Technology. ISSN 0974-3154, Volume 12, Number 8 (2019), pp. 1263-1268

Identification of the Phase Composition of Dental Ceramic Materials

K. D. Altynbekov[1], B. Zh. Nysanova[1], L. P. Antonova[2], Ye. A. Berdimbetov[3], K. M. Smagulov[3]

[1] *Department of Prosthetic dentistry, Asfendiyarov Kazakh National Medical University, Almaty - 050012, Almaty Region, Kazakhstan.*

[2] *Department of Stomatology, LLP "Educational and Medical Enterprise Daris-TTE", Almaty - 050016, Almaty Region, Kazakhstan*

[3] *Department of Stomatology, Karaganda State Medical University, Karaganda - 100000, Karaganda Region, Kazakhstan.*

Abstract:

This paper is devoted to the identification of phase changes in dental ceramic masses such as Duceram plus and Noritake EX3 before and after repeated firing in compliance with the manufacturers' instructions using the methods of X-ray phase (XRF) and differential thermal (DTA) analyses. The regularities of changes in the phase composition of glass-ceramic masses for metal-ceramic dentures occurring in the firing process were studied. As a result of an experimental study, we determined the factors leading to an increase in the glass phase content (the area of the halo increases, and it becomes sharp), the β-cristobalite (SiO2) to X-quartz transition, the appearance of albite crystals, as well as the disappearance of calcium and phosphorus-containing individuals. Glass-ceramic dental materials are mainly represented by solid solutions. It should be emphasized that the identification of the phase composition of lining porcelain materials requires further research using physico-chemical analysis and microstructure.

Keywords - glass ceramics, X-ray phase analysis, alloy.

I. INTRODUCTION

Currently, polymers, composites, compomers, and ceramic materials are used for manufacturing the facing layer of denture constructions [1-4]. One of the leading places in orthopedic dentistry is occupied by studies of the physicomechanical and chemical characteristics of dental porcelain for metal ceramics [5]. Metal-ceramic denture constructions have an advantage over plastic ones, since they fully meet the medical and technical requirements imposed on them.

The properties of ceramics, such as biocompatibility, aesthetics and durability, the ease of making complex shapes, as well as sufficient mechanical and corrosion resistance were analyzed by Popkov et al. (2006), Bolotnaya (2006), Dyakonenko and Lebedenko (2016), and Arutyunov (1990) [6–9]. Most studies focus on the physical properties of ceramics, while few are devoted to examining the crystal features of glass-ceramic masses, the patterns of change in the phase composition during firing, and the stability of materials during multiple firing [10–13]. Much attention is paid to microscopic methods for studying glass-ceramic materials, which allow us to determine the quantitative and qualitative characteristics of the crystal component of glass-ceramics.

According to the available data, when identifying the crystal chemical characteristics of materials, the main role is assigned to spectral changes of the phase composition by research methods such as emission spectral, X-ray fluorescence and microprobe X-ray analyses. This allows us to identify and characterize the morphological features of ceramic masses [14, 15].

Deviations from the firing temperature mode can lead to a violation of surface and bulk crystallization, as well as a change in the ratio of the crystalline phase to the glass phase, which results in internal stress in the lining and microcracks [16]. In this regard, the identification of the phase composition of dental ceramic materials using X-ray phase (XRF) and differential thermal (DTA) analyses are of particular interest.

II. MATERIALS AND METHODS

Two imported lining glass-ceramic materials, which constitute a large part among those used in Kazakhstan for metal-ceramic dentures, were investigated: Duceram Plus – of natural origin (Germany), and Noritake EX3 – of synthetic origin (Japan).

To study the possible changes in the crystal composition during heat treatment, to compare the phase composition on the sample surface and in the volume, as well as to assess stability during repeated firing, the samples were divided into two groups.

The first group of materials consisted of initial enamel and dentin powders, as well as silica clay suspensions or powders. The second group of materials consisted of sintered glass-ceramic samples on substrates of Stomet-1 kz and Stomet-2 kz alloys, enamel, dentin and silica clay followed by triturating. Sample sintering was carried out in a Programet P90 (Ivoclar, Vivadent, Liechtenstein) electrovacuum furnace strictly following the manufacturers' instructions.

X-ray phase analysis (XRF) was carried out on a DRON-3M diffractometer on CuKα radiation. X-ray diffraction patterns were obtained in the range of angles of 10 to 70 degrees.

The decoding of X-ray diffraction patterns was to determine the values of the interplanar distances (d) and the relative intensity of the reflections (I rel). In this work, X-ray phase analysis was carried out to study the composition of ceramic masses.

The samples were prepared as follows: first, they were powdered in an agate mortar, then the powder was poured into a Plexiglas cuvette, pre-smeared with petroleum jelly and

slightly pressed, and the excess powder was cut off with a blade to eliminate the texture.

The identification of various phases based on the diffraction pattern analysis was carried out by the set of its interplanar distances and relative intensities of the corresponding lines on the X-ray diffraction pattern. Differential-thermal analysis was carried out on "Derivatograph Q-1500D" made by MOM in the following order. The samples were powdered in an agate mortar, then the test substance was poured into a crucible; thermograms were taken at 1000°C at a heating rate of 10°C per minute. A comparative characteristic of XRF and DTA analyses was given in the framework of the standard study design [16-18]. The obtained spectra were interpreted using a computer program based on an automated system for reading and processing of radiographic information according to the Joint Committee on Powder Diffraction Standards.

III. RESULTS

1) XRF Results

According to the XRF analysis of a sample of powdered silica clay (Duceram plus) before firing, the study revealed the presence of a feldspathic individual of leucite composition with the interplanar distances (d Å): leucite ($K(AlSi_2O_6)$): 5,38; 5,50; 4,73; 3,34; 3,27; 3,05; 2,64; 2,36; 2,30; 2,14; 1,65; 1,47, and minerals with the interplanar distances (d, Å): dolomite ($CaMg(CO_3)_2$): 2,92; 2,18; 2,07; 1,76; 1,38, β-cristobalite (β-SiO_2): 4,06; 3,14; 2,83; 1,91; 1,51; 1,41, α-quartz (α-SiO_2): 4,43; 3,42; 2,52; 1,83; 1,71; 1,59; 1,43.

The XRF analysis of Noritake EX3 silica clay mass before firing showed the presence of leucite ($KAlSi_2O_6$) with the interplanar distances (d, Å): 5,40; 4,75; 3,44; 3,27; 2,92; 2,84; 1,65, and mineral impurities with the interplanar distances (d, Å): cerianite (CeO_2) – 3,12; 2,70; 1,91; 1,63, zircon ($ZrSiO_4$) - 4,45; 3,31; 2,52; 1,71, corundum (α-Al_2O_3) – 2,55; 2,37; 2,07; 1,60; 1,38, and hematite (α-Fe_2O_3) – 2,46; 2,22; 1,47; 1,44; 1,35.

According to the XRF analysis of Ceram Bond silica clay mass, in the form of an emulsion, the study revealed the presence of minerals with the interplanar distances (d, Å): kaolinite ($Al_2(Si_2O_5)$) – 3,57; 2,35; 1,48, dickite ($Al_2O_3{\cdot}2SiO_2{\cdot}2H_2O$) – 7,89; 4,97; 4,09; 3,30; 2,40; 1,51, hematite (α-Fe_2O_3) – 2,67; 2,17; 1,90; 1,46; 1,44; 1,36, and β-quartz (β-SiO_2) – 2,45; 1,77, 1,71; 1,67.

By performing the XRF analysis of Duceram plus dentin mass before firing, the study revealed the presence of feldspar glass of leucite composition with the interplanar distances (d, Å): leucite ($K(AlSi_2O_6)$): 5,66; 5,40; 3,43; 3,28; 2,93; 2,36; 1,66, and the presence of minerals in the form of impurities with the interplanar distances (d, Å): calcium orthophosphate ($Ca_3(PO_4)_2$): 3,67; 2,89; 2,64; 2,59; 1,71, magnesium orthophosphate ($Mg_3(PO_4)_2$): 2,41; 2,13; 2,04, calcite ($CaCO_3$): 3,03; 1,91; 1,87, dolomite ($CaMg(CO_3)_2$): 2,84; 2,19, tricalcium phosphate ($3CaO{\cdot}P_2O_5$): 3,22, β-cristobalite (SiO_2): 4,01; 3,12; 1,86, and wollastonite (β-$CaO{\cdot}SiO_2$): 7,89; 3,81; 3,51; 3,31; 2,97; 2,47; 2,18; 1,83.

The XRF analysis of Noritake EX3 dentin mass before firing showed the presence of feldspar crystal leucite composition with the interplanar distances (d, Å): leucite ($K(AlSi_2O_6)$: 5,38; 4,72; 3,43; 3,27; 2,92; 1,66, and minerals with the interplanar distances (d, Å): podolite ($Ca_{10}(PO_4)_6(CO_3)$): 2,81; 2,77; 2,71; 2,25; 1,9, β-cristobalite (SiO_2): 4,08; 3,15; 2,48, wollastonite (β-$CaO{\cdot}SiO_2$): 7,9; 3,83; 3,59; 2,98; 2,46; 2,28; 2,18; 1,83, yttrium oxide (Y_2O_3): 3,04; 1,87; 1,60, and zirconium oxide (ZrO_2): 2,84; 1,84; 1,81.

After applying Duceram plus ceramic mass (silica clay, dentin) to the metal frame of Stomet 1 kz alloy in compliance with the firing process technologies, the XRF analysis showed the presence of minerals in the form of impurities with the interplanar distances (d, Å): nontronite (Fe^{3+}, Fe^{2+}, Mg, $Al)_2O_3{\cdot}4SiO_2{\cdot}H_2O{\cdot}\ mH_2O$) – 3,2837; 1,7281; 1,5378; 1,4958, montmorillonite ($Al,\ Mg)_2\ (OH)_2\ {\cdot}[Si_4O_{10}]\ {\cdot}H_2O$) – 2,4532; 2,1374; 1,6741, goethite ($HFeO_2$) – 5,0245; 1,9107; 1,8057, and γ–tridymite (γ SiO_2) – 3,4309; 2,0878.

After applying Noritake EX3 ceramic mass (silica clay, dentin) to the metal frame of Stomet 1 kz, the XRF analysis revealed the presence of minerals in the form of impurities with the interplanar distances (d, Å): actinolite ($Ca_2\ (Mg,Fe)_5{\cdot}[Si_8O_{22}]\ {\cdot}\ (OH)_2$ –3,2853; 2,9379, illite $K<\ (Al,Fe)_2\ [OH]_2\ Al\ Si_3O_{10}]\ nH_2O$ –3,7264; 3,4446; 1,5001, sepiolite ($Mg_3\ [Si_4O_{11}]\ {\cdot}nH_2O$) – 7,8933; 2,2962; 1,8043; 1,7333; 1,5292, and microcline ($K_2\ O\ {\cdot}Al_2\ O_3\ {\cdot}6SiO_2$) – 2,3258; 1,8511; 1,4808; 1,4214.

Based on the XRF analysis, after firing Duceram plus ceramic mass (silica clay, dentin) on the metal frame of Stomet-2 kz alloy, the study showed the presence of minerals in the form of impurities with the interplanar distances (d, Å): microcline ($K_2\ O\ {\cdot}Al_2\ O_3\ {\cdot}6SiO_2$) –3,77; 2,92; 1,38, actinolite ($Ca_2\ (Mg,Fe)_5{\cdot}[Si_8O_{22}]\ {\cdot}\ (OH)_2$ –3,28; 1,433, tremolite – ($2Ca\ O{\cdot}5MgO{\cdot}8SiO_2{\cdot}\ H_2O$)- 1,4924; 1,845; 1,9668, and monotermite ($0{,}2RO\ {\cdot}Al_2\ O_3\ {\cdot}3SiO_2\ {\cdot}\ 1{,}5\ H_2O(+0{,}5H_2O)$ – 2,06;1,71; 1,53.

The XRF analysis, carried out after applying Noritake EX3 ceramic mass (silica clay, dentin) on the metal frame of Stomet 2 kz alloy, revealed the presence of minerals in the form of impurities with the interplanar distances (d, Å): mono-thermite ($0{,}2RO\ {\cdot}Al_2\ O_3\ {\cdot}3SiO_2\ {\cdot}\ 1{,}5\ H_2O(+0{,}5H_2O)$ – 3,4346; 1,9769; 1,715; 1,6014; 1,5362; 1,4837, halloysite ($Al_2O_3{\cdot}2SiO_2{\cdot}4H_2O$) – 2,2229; 2,4926, pyrophylite ($Al_2O_3{\cdot}4SiO_2{\cdot}H_2O$) – 4,0879; 1,9127; 1,6738; 1,3823, and β-albite ($Na_2O\ {\cdot}Al_2O_3{\cdot}6SiO_2$) - 3,2797; 2,0514; 1,8007.

After firing Duceram plus ceramic mass (silica clay, dentin, porcelain enamel) on the metal frame of Stomet 1 kz, the XRF analysis showed the presence of leucite ($KAlSi_2O_6$) with the interplanar distances (d, Å): 1,9189; 1,4401, and mineral impurities with the interplanar distances (d, Å): calcite ($CaCO_3$): 2,4962; 1,8741; 1,5233; 1,3550, goethite ($HFeO_2$) – 1,8043; 1,7279; 1,4242, mullite ($3Al_2O_3{\cdot}SiO_2$) – 5,4402; 3,7627; 2,2072; 1,8486, montmorillonite ($Al,\ Mg)_2\ (OH)_2\ {\cdot}[Si_4O_{10}]\ {\cdot}H_2O$) – 4,0573; 1,6771; 1,5598, and monotermite ($0{,}2RO\ {\cdot}Al_2\ O_3\ {\cdot}3SiO_2\ {\cdot}\ 1{,}5\ H_2O(+0{,}5H_2O)$ – 1,9779; 1,7925; 1,5366; 1,3677.

After applying Noritake EX3 ceramic mass (silica clay, dentin, porcelain enamel) to the metal frame of Stomet 1 kz in compliance with the firing process technologies during the

XRF analysis, the study revealed the presence of leucite ($KAlSi_2O_6$) with the interplanar distances (d, Å): 5,843; 4,7537; 1,5301, and mineral impurities with the interplanar distances (d, Å): calcite ($CaCO_3$): 2,4926; 2,2415; 1,3550, goethite ($HFeO_2$) – 5,0207; 1,9146; 1,8054; 1,4209, mullite ($3Al_2O_3 \cdot SiO_2$) – 5,4082; 3,7626; 1,8444, illite K< (Al,Fe) $_2$ [OH]$_2$ Al Si_3O_{10}] nH_2O – 3,4441; 2,5652; 2,4464; 1,5076, β-albite ($Na_2O \cdot Al_2O_3 \cdot 6SiO_2$) - 3,1316; 2,5189; 2,1657;1,7327; 1,5146; 1,4411, montmorillonite (Al, Mg)$_2$ $(OH)_2$ $\cdot[Si_4O_{10}] \cdot H_2O$) – 6,4670; 2,1360, and actinolite $(Ca_2 (Mg,Fe)_5 \cdot [Si_8O_{22}] \cdot (OH)_2$ – 3,9286; 3,2856.

Duceram plus ceramic mass (silica clay, dentin, porcelain enamel) on the metal frame of Stomet 2 kz was found with leucite ($KAlSi_2O_6$) with the interplanar distances (d, Å): 1,9191; 1,4409, and mineral impurities with the interplanar distances (d, Å): calcite ($CaCO_3$): 1,8704; 1,3550, goethite ($HFeO_2$) – 5,0606; 2,0914; 1,8007, mullite ($3Al_2O_3 \cdot SiO_2$) – 5,4060; 1,8405, monotermite ($0{,}2RO \cdot Al_2O_3 \cdot 3SiO_2 \cdot 1{,}5 H_2O(+0{,}5H_2O)$ – 3,4316;2,0694;1,5382, illite K< (Al,Fe) $_2$ [OH]$_2$ Al Si_3O_{10}] nH_2O –2,8438; 2,5610; 1,9898; 1,6424; 1,3860, and nontronite (Fe^{3+}, Fe^{2+}, Mg, Al)$_2O_3 \cdot 4SiO_2 \cdot H_2O \cdot mH_2O$) – 3,2848; 1,720.

After firing Noritake EX3 ceramic mass (silica clay, dentin, porcelain enamel) on the metal frame of Stomet 2 kz in compliance with the firing process technologies, the XRF analysis revealed the presence of mineral impurities with the interplanar distances (d, Å): leucite ($KAlSi_2O_6$) – 5,881; 4,085; 3,644; 1,785; 1,588; 1,534; 1,402; 1,355, and mineral impurities with the interplanar distances (d, Å): goethite ($HFeO_2$) – 5,0964; 1,9111, montmorillonite (Al, Mg)$_2$ $(OH)_2$ $\cdot[Si_4O_{10}] \cdot H_2O$) – 6,4914;1,2,1359;1,4990; 1,3811, monotermite ($0{,}2RO \cdot Al_2O_3 \cdot 3SiO_2 \cdot 1{,}5 H_2O(+0{,}5H_2O)$ – 3,4325; 2,0680; 1,7187; 1,4021, α-β cristobalite (SiO_2): 2,4893; 2,0206; 1,5347, β-albite ($Na_2O \cdot Al_2O_3 \cdot 6SiO_2$) - 3,2742; 2,4180; 2,2401;1,4211, β-quartz (β-SiO_2) – 4,2558; 1,6648, 1,4591, and α-tritimite (α SiO_2) – 4,0852; 2,0893; 1,8486.

A comparison of the X-ray diffraction patterns of Duceram plus dentin masses of the studied samples (Fig. 1 and Fig. 2) before and after firing shows that an additional firing of the mixture leads to an increase in the glass phase content, the β-cristobalite to α-quartz transition, the appearance of albite crystals, as well as the disappearance of calcium and phosphorus-containing individuals. The fact that leucite is represented in the glass-crystallite form is indicated by the appearance of a halo on the X-ray diffraction pattern in the region from 5.2729 to 2.5938. The presence of free β-cristobalite SiO_2 in the dentin composition may cause hidden microcracks on dentin.

Fig. 1. The X-ray diffraction pattern of Duceram plus dentin mass before firing

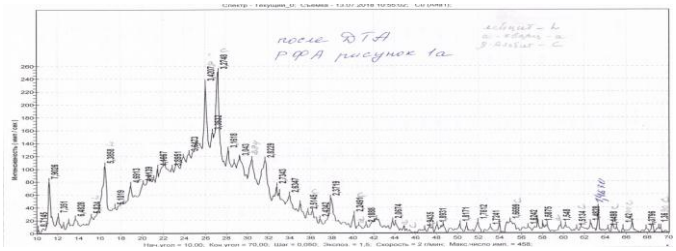

Fig.2. The X-ray diffraction pattern of Duceram plus dentin mass after firing

2) DTA Results

The DTA curve of Duceram plus powdery silica clay mass shows the following endoeffects and exoeffects:

(+) 117ºC – β-cristobalite inversion (SiO_2);

(–) 610ºC – dissociation of calcium and magnesium carbonates;

(+) 920ºC – crystallization of feldspar glass.

The DTA curve of Noritake EX3 silica clay mass (Fig. 3) shows the following endoeffects and exoeffects:

(+) 378ºC and (+) 423ºC – oxidation of organic impurities;

(–) 555ºC – removal of constitutional water from impurity diaspore.

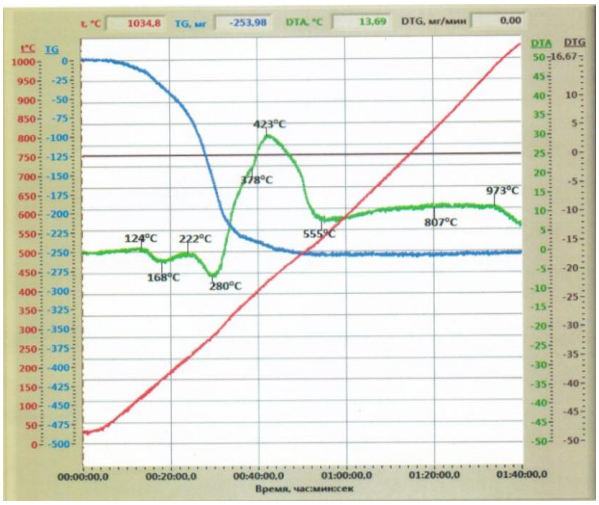

Fig. 3. The DTA curve of Noritake EX3 silica clay mass

The DTA curve of Ceram Bond silica clay mass (Fig. 4) shows the following endoeffects and exoeffects:

(+) 143ºC and 221ºC – removal of sorbed water, whose presence is associated with a high specific surface area of the particles that is usually directly dependent on the disordering of kaolinite structure;

(–) 463ºC and 559ºC – extraction of constitutional water with destruction of the crystal lattice;

(+) 978ºC – crystallization of mullite and γ = Al_2O_3.

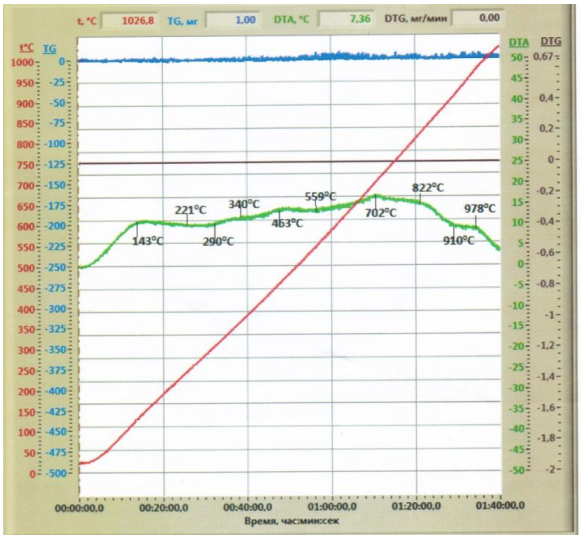

Fig. 4. The DTA curve of Ceram Bond silica clay mass

The DTA curve of Duceram plus dentin mass (Fig. 5) shows the following endoeffects and exoeffects:

(+) 114°C – β-cristobalite inversion (SiO_2);

(-) 361°C – phosphate hydration;

(-) 600–800°C – dissociation of calcium and magnesium carbonates;

(-) 900°C – crystallization of feldspar glass.

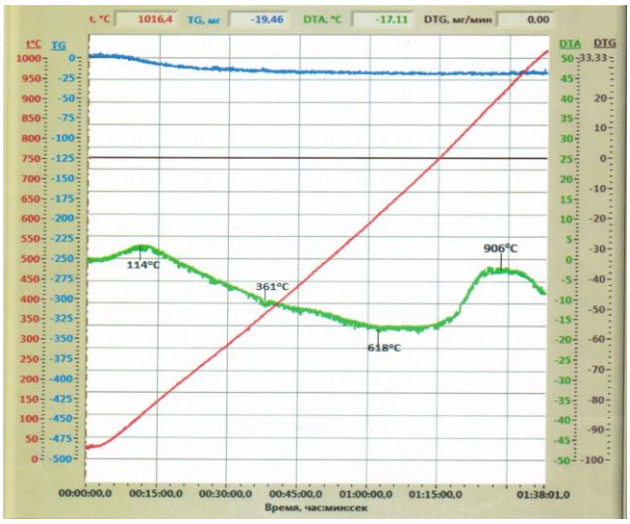

Fig. 5. The DTA curve of Duceram plus dentin mass

The DTA curve of Noritake EX3 dentin mass (Fig. 6) shows the following endoeffects and exoeffects:

(+) 118°C – β-cristobalite inversion (β-SiO_2);

(-) 350°C – phosphate hydration;

(-) 553°C – reversible polymorphic transformation to α-quartz (α-SiO_2);

(-) 794°C – dissociation of calcium and magnesium carbonates;

(+) 915°C – crystallization of feldspar glass.

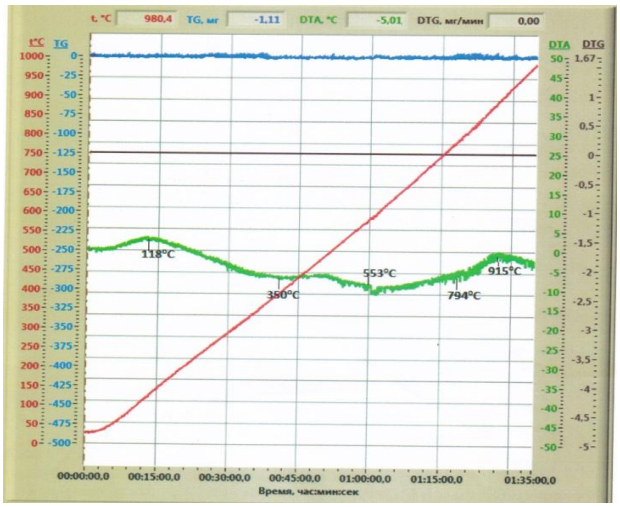

Fig. 6. The DTA curve of Noritake EX3 dentin mass

IV. DISCUSSION

Based on XRF and DTA results, phase compositions were determined.

A comparison of the X-ray diffraction pattern of the ceramic mass of the studied samples before and after firing shows that an additional firing of the mixtures leads to an increase in the glass phase content, the β-cristobalite to α-quartz transition, the appearance of albite crystals, as well as the disappearance of calcium and phosphorus-containing individuals.

A comparison of the X-ray diffraction pattern of the dentin mass before and after firing shows that an additional firing of the mixtures leads to an increase in the glass phase content (the area of the halo increases, and it becomes sharp); the β-cristobalite (SiO_2) to x-quartz transition, the appearance of albite crystals ($Na_2O \cdot Al_2O_3 \cdot 6SiO_2$), as well as the disappearance of calcium and phosphorus-containing individuals. The XRF and DTA of the ceramic masses of Duceram Plus (of natural origin) and Noritake EX3 (of synthetic origin) showed different phase changes, which, apparently, connect their origin, chemical difference, structure and composition.

According to the data, the porcelain mass of synthetic origin in contrast to the feldspar, i.e. of natural origin, contains significantly smaller leucite, distributed in a glass matrix more tightly and evenly. At the same time, it is known that leucite crystals inhibit the formation of microcracks in the less durable amorphous glass phase. This provides a higher mechanical strength of porcelain and its resistance to thermal effects [19].

Most studies have proved that the more leucite in porcelain and the smaller the size of its crystals, the higher its strength and optical properties. The same phase composition is characteristic of porcelain masses, such as IPS-Classic, Duceram plus, Noritake EX3, in which the thermal expansion is 13.1-14.3*10k, allowing them to be successfully used in

combination with Co-Cr alloys with the coefficient of thermal expansion of 13.8-14.410k.

Leucite crystals have a higher coefficient of linear thermal expansion than the rest of the glass matrix, so the latter is under compression stress, while leucite crystals are subjected to tensile forces. Consequently, compression stresses arise at the interface between the leucite and matrix crystals, preventing the development of cracks [20].

As a result of the qualitative analysis of the microstructures of the samples by the X-ray structural method, it was found that the main crystalline phase of Duceram plus and Noritake EX3 is leucite, which gives ceramics stability. A comparative analysis of the diffraction patterns obtained during the study before and after firing of Duceram plus mass revealed the identity of the glass-crystalline structures, which is consistent with other studies. A similar pattern is observed in Noritake EX3 mass.

The fact that leucite is represented in the glass-crystallite form is indicated by the appearance of a halo on the X-ray diffraction pattern in the region from 5.2729° to 2.5938°. The presence of free β-cristobalite SiO_2 in the dentin composition may cause hidden microcracks on dentin.

The identification of the phase composition using DTA showed some endoeffects and exoeffects fixed on the DTA curve of Noritake EX3 dentin mass:

(+) 147°C – β-cristobalite inversion (β-SiO_2);

(-) 355°C – phosphate hydration;

(-) 656°C – reversible polymorphic transformation to α-quartz (α-SiO_2);

(-) 739°C – dissociation of calcium and magnesium carbonates;

(+) 930°C – crystallization of feldspar glass.

Similar endoeffects are observed when carrying out the DTA of kaolin formed mullite [22].

The XRF analysis of Noritake EX3 dentin mass before firing revealed the presence of feldspathic crystalline leucite composition with the interplanar distances (d, Å): leucite ($K(AlSi_2O_6)$): 5,38; 3,43; 3,26; 1,66, and minerals with the interplanar distances (d, Å): pyromorphite ($Pb_5(PO_4)_3Cl$): 2,92; 2,78; 2,37; 2,13; 2,02; 1,95; 1,91; 1,52; 1,47, β-cristobalite (SiO_2): 4,09; 3,14; 2,84; 2,48, yttrium oxide (Y_2O_3): 3,08; 1,87; 1,81, and zirconium oxide (ZrO_2): 3,18; 2,84.

X-ray spectral analysis allows us to determine not only the quantitative and qualitative macroelement and microelement composition of the material, but also to map the primary distribution of ions on the sample surface [23].

V. CONCLUSIONS

The identification of phase changes was considered in dental ceramic masses such as Duceram plus and Noritake EX3 before and after repeated firing in compliance with the manufacturers' instructions using the methods of X-ray phase (XRF) and differential thermal (DTA) analyses.

Based on the results of X-ray phase, differential thermal and chemical X-ray fluorescence analyses, phase compositions were established.

A comparison of the X-ray diffraction patterns of the ceramic mass of the studied samples before and after firing revealed that an additional firing of the mixtures leads to an increase in the glass phase content, the β-cristobalite to α-quartz transition, the appearance of albite crystals, as well as the disappearance of calcium and phosphorus-containing individuals.

Currently, metal ceramic products, i.e. glass-ceramic coatings based on feldspar glass, are widely used in prosthetic dentistry. Glass ceramics consists of silicon oxide, also known as quartz (SiO_2) with a low aluminum content. Aluminosilicates, which also contain potassium and sodium impurities, are biologically known as feldspar.

During X-ray diffraction analysis, the crystalline phase of leucite is identified in fired dental ceramics. The presence of leucite in the phase composition is a distinctive feature of dental ceramics, since such crystalline phase is absent in household porcelain. The presence of leucite in dental ceramics is due to the use of potassium feldspar as an initial component. Leucite in porcelain is formed during the thermal decomposition of potassium feldspar: $K_2O{\cdot}Al_2O_3{\cdot}6SiO_2 \rightarrow K_2O{\cdot}Al_2O_3{\cdot}4SiO_2+2SiO_2$, while SiO_2 dissolves in the resulting glass, increasing the melt viscosity. Leucite crystals in the form of globules, evenly and in large quantities distributed in a glass matrix, prevent the spread of cracks and thereby increase the strength of porcelain. In addition, leucite crystals, unlike mullite (the crystalline phase of household porcelain), are characterized by transparency.

Glass-ceramic dental materials are mainly represented by solid solutions. It should be emphasized that the identification of the phase composition of lining porcelain materials requires further research using physico-chemical analysis and microstructure.

REFERENCES

[1] N. J. Opdam, E. M. Broakhorst, B. A. Loomans, and M. C. Huysmans, 12 Year survival of composite vs amalgam restorations, Journal of dental research 89, 2010, 1063-1067.

[2] A. Barone, G. Derchi, A. Rossi, S. Marconni, and V. Covani, Longitudinal clinical evaluation of bonded composite inlays, Quintessence International 39, 2008, 65-71.

[3] P. F. Manicone, R. Lometti, and L. Rafaelli, An overview of zirconia ceramics-basic properties and clinical application, Journal of dentistry, 35, 2007, 819-826.

[4] A. Jotkowitz, N. Samet, and V. Rethinsky, Ferule a new approach to an old dilemma, British Dental Journal, 209, 2001, 25-33.

[5] E. A. Kulinich, Compositions and technology of leucite-hydroxyapatite fluorite coatings for dentistry and

medical devices. The author's summary of doctoral dissertation (Tomsk, 2005).

[6] V. A. Popkov, O. V. Nesterova, V. Yu. Reshetnyak, and I. N. Avertseva, Dental material science [Textbook] (Moscow: MEDpress-inform, 2006).

[7] V. N. Bolotnaya, Long-term results of orthopedic treatment with metal-ceramic prosthetic bridges: The author's summary of doctoral dissertation. (Irkutsk, 2006).

[8] E. E. Dyakonenko, and I. Yu. Lebedenko, World trends in the study of dental ceramic materials, Journal of Dental Materials, Dentistry, 5, 2016, 61-68.

[9] S. D. Arutyunov, Prevention of complications in the use of metal-ceramic dentures. The author's summary of doctoral dissertation (Moscow, 1990).

[10] D. E. Parsell, and K. J. Anusavice, Optimization of glass-ceramic crystallization based on dta exotherm analysis. Dent. Mater, 10(3), 1994, 167-171.

[11] I. Yu. Lebedenko, Yu. B. Makarychev, V. N. Kopeikin, Yu. L. Anisimov, and V. A. Kozlov, The study of the contact area of the coating with the frame of metal-ceramic dentures, Problems of Neurodentistry and Dentistry, 1, 1998, 18-25.

[12] Yu. A. Shirokova, Metal-ceramic dentures based on zirconium alloy frames. Doctoral dissertation (Moscow, 2002).

[13] V. F. Khetagurov, The use of microplasma processing in the manufacture of metal-ceramic dentures. Doctoral dissertation (Moscow, 2004).

[14] R. Trushkowsky, Porcelain fracture: cfuses, prevention, fnd repair techniques. J. Mass. Dent. Soc., 41(l), 1992, 29-34.

[15] S. V. Kharitonov, The technology of manufacturing metal-ceramic constructions in the clinic of prosthetic dentistry and forensic medicine (Moscow: MSUMD, 2004).

[16] W. W. Wendlandt, Thermal methods of analysis (Moscow: Mir, 1978).

[17] W. Hemminger, and G. Höhne, Calorimetry: Fundamentals and practice (Moscow: Chemistry, 1989).

[18] I. B. Shatalov, O. A. Shlyakhtin, and E. Veryaeva, Methods of thermal analysis (Moscow, 2011).

[19] V. N. Batin, S. A. Gorban, and R. Kh. Kamalov, Study of the composition of a new synthetic ceramic mass (Moscow, 2002).

[20] J. T. Jones, and M. F. Berard, Ceramics: Industrial Processing and Testing (Ames IA: The Iowa State University Press).

[21] K. G. Ewsuk, "Effects of Trapped Gases on Ceramic-Filled-Glass Composite Densii3cation," in Solid State Phenomena, Vol. 25-26, Sintering' 91, edited by A. C. D. Chaklader and J. A. Lund, Trans Tech Publications Ltd., Brookileld, VT, 1992, pp. 63-72.

[22] F. Sahnoune, M. Chegaar, N. Saheb, Differential thermal analysis of mullite formation from Algerian kaolin. *in* Advances in Applied Ceramics 107(1):9-13, February 2008.

[23] D. W. Richerson, Modern Ceramic Engineering: Properties, Processing, and Use in Design, second edition, Marcel Dekker, Inc., New York, 1992.